Since January 2020 Elsevier has created a COVID-19 resource centre with free information in English and Mandarin on the novel coronavirus COVID-19. The COVID-19 resource centre is hosted on Elsevier Connect, the company's public news and information website.

Immunology Letters 242 (2022) 1–7

Contents lists available at ScienceDirect

Immunology Letters

journal homepage: www.elsevier.com/locate/immlet

A novel antibody against the furin cleavage site of SARS-CoV-2 spike protein: Effects on proteolytic cleavage and ACE2 binding

Michael G. Spelios [a], Jeanne M. Capanelli [a], Adam W. Li [a,*]

[a] EpiGentek Group Inc., 110 Bi County Boulevard, Suite 122, Farmingdale, NY, 11735, United States of America

ARTICLE INFO

Keywords:
SARS-CoV-2
COVID-19
Spike
Furin
Proprotein convertase
ACE2
Furin site blocking antibody

ABSTRACT

SARS-CoV-2 harbors a unique S1/S2 furin cleavage site within its spike protein, which can be cleaved by furin and other proprotein convertases. Proteolytic activation of SARS-CoV-2 spike protein at the S1/S2 boundary facilitates interaction with host ACE2 receptor for cell entry. To address this, high titer antibody was generated against the SARS-CoV-2-specific furin motif. Using a series of innovative ELISA-based assays, this furin site blocking antibody displayed high sensitivity and specificity for the S1/S2 furin cleavage site, including with a P681R mutation, and demonstrated effective blockage of both enzyme-mediated cleavage and spike-ACE2 interaction. The results suggest that immunological blocking of the furin cleavage site may afford a suitable approach to stem proteolytic activation of SARS-CoV-2 spike protein and curtail viral infectivity.

1. Introduction

Severe acute respiratory syndrome coronavirus 2 (SARS-CoV-2) was first recognized in the beginning of 2020 and is responsible for the present COVID-19 pandemic [1]. SARS-CoV-2 consists of a positive-sense single-stranded RNA genome and 4 different types of structural proteins [2]. The N, or nucleocapsid, protein encapsidates the genome, while the S (spike), E (envelope), and M (membrane) proteins comprise the surrounding lipid bilayer envelope. Of particular appeal is the S protein, which enables viral infection via angiotensin-converting enzyme 2 (ACE2) receptor recognition and membrane fusion, making this structural protein an ideal target for therapeutic intervention.

The S protein is composed of two subunits, S1 and S2. Within the S1 subunit is a receptor-binding domain (RBD) that recognizes and binds to the ACE2 receptor [3]. The S protein also harbors a furin cleavage site at the boundary between the subunits [4]. The complete SARS-CoV-2 furin cleavage site has been characterized as a 20 amino acid motif corresponding to the amino acid sequence ^{A}672-^{S}691 of SARS-CoV-2 spike protein (Fig. 1), with one core region SPRRAR|SV (8 amino acids, ^{S}680-^{V}687) and two flanking solvent-accessible regions (8 amino acids, ^{A}672–^{N}679, and 4 amino acids, ^{A}688-^{S}691) [5,6]. The core region is very unique as its ^{R}683 and ^{A}684 positions are positively-charged (Arg) and hydrophobic (Ala) residues, respectively, which could be cleaved by the proprotein convertase (PC) furin and/or furin-like PCs secreted from host cells and bacteria in the airway epithelium [7]. A ^{R}683 site mutation to ^{Q}683 is one of several key modifications incorporated into a current protein-based vaccine candidate, which stabilizes the S protein antigen in its prefusion form by rendering it protease resistant [8,9]. The ^{P}681 site mutating to ^{R}681 was observed in the Delta variant and shown to cause higher infection and transmission [10]. Interestingly, a deletion variant with all arginines in the core region excluded did not affect virus replication in vitro, despite a prospective loss of furin cleavage susceptibility [11].

Furin and furin-like PCs, such as PC5/6A and PACE4, are proven to be cleavage region sequence-specific, and these PCs exhibit widespread tissue distribution [12]. With this unique furin cleavage site, such distribution may explain why COVID-19 causes damage in multiple organs. Thus, the importance of blocking SARS-CoV-2 S1/S2 site cleavage caused by furin or facilitating protease activity is emphasized by the fact that cleavage of the S protein at the S1/S2 site has been documented as essential for SARS-CoV-2 binding to the host ACE2 receptor, cell-cell fusion, and infection of human lung cells [13,14].

Due to the correlation between PC-mediated cleavage and S protein activation, we hypothesized that blockage of the furin cleavage site could potentially subvert SARS-CoV-2 infection by hindering enzymatic action and S protein-ACE2 interaction. To address this, we generated a novel antibody with high sensitivity and specificity for the furin cleavage site of SARS-CoV-2 spike protein. The antibody was then employed in a series of innovative in vitro assays where it was observed to efficiently block a) cleavage by purified enzymes and human specimens,

* Corresponding author.
E-mail address: awli@epigentek.com (A.W. Li).

https://doi.org/10.1016/j.imlet.2022.01.002
Received 17 May 2021; Received in revised form 5 January 2022; Accepted 6 January 2022
Available online 7 January 2022

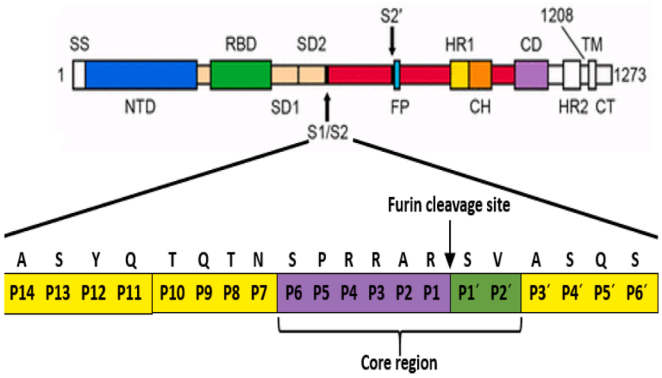

Fig. 1. Schematic of the SARS-CoV-2 spike protein, including the location of the furin cleavage site at the boundary between the S1 and S2 subunits.

and b) binding to ACE2. To our knowledge, this is the first time that such an antibody-based tactic directed against the target of SARS-CoV-2-specific PC activity has been established.

2. Materials and methods

2.1. Generation of furin site blocking antibody (fbAB)

Antigen consisted of the SARS-CoV-2-specific furin motif (20 aa; Fig. 1) conjugated to keyhole limpet hemocyanin (KLH). The peptide-KLH conjugate (0.5 mg) was injected into a New Zealand White rabbit with Freund's adjuvant, followed by a boost (3 × 0.25 mg) over 2 weeks. Serum was collected 1 week post-boost and antibody was purified with SulfoLink protein A columns (ThermoFisher Scientific).

2.2. Quantification of fbAB titer

To test the titer of the generated fbAB, the antigen was coated onto high protein binding, polystyrene, 8-well microplate strips (Greiner) at a concentration of 200 ng/well with 0.1 M $NaCO_3$. The strips were incubated for 2 h at 37 °C for coating and then blocked with 2% BSA (in PBS) for 1 h at 37 °C. After washing the strips for 3 times with PBS containing 0.1% Tween 20 (PBS-T), fbAB was added into the wells at the indicated dilutions (prepared with PBS-T) and incubated for 1 h at RT. After washing for 4 times, anti-rabbit IgG-HRP (EpiGentek) (50 μl, 1:2000 dilution in PBS-T) was added and incubated for 30 min at RT. After washing for 4 times, 100 μl of TMB solution (EMD Millipore Corp.) were added per well and blue color development was monitored for 2–10 min. The reaction was stopped with an equal volume of 1 M HCl and the optical density was measured with a microplate reader (MRX-TC Revelation, Dynex Technologies) at a wavelength of 450 nm.

2.3. Sensitivity of fbAB recognition

A SARS-CoV-2 protein (Sino Biological), containing the S1/S2 boundary furin site and tagged with polyhistidine (His) at the N-terminal, was added at different concentrations (0.01 - 100 ng/well, prepared with PBS) into blocked (2% BSA) nickel-nitrilotriacetic acid (Ni-NTA)-coated polystyrene, 8-well microplate strips (Fisher) and incubated for 45 min at RT. After washing the strips for 2 times with PBS-T, fbAB (50 μl, 1:2000 dilution in PBS-T) was added and incubated for 1 h at RT. After washing for 3 times, anti-rabbit IgG-HRP (50 μl, 1:2000 dilution in PBS-T) was added and incubated for 30 min at RT. After washing for 4 times, 100 μl of TMB solution were added per well and blue color development was monitored for 2–10 min. The reaction was stopped with an equal volume of 1 M HCl and the optical density was measured with a microplate reader at a wavelength of 450 nm.

2.4. Specificity of fbAB recognition

His-tagged SARS-CoV-2 protein containing the S1/S2 boundary furin site, His-tagged peptides containing the wild type, mutant (P681R and R683Q), and triple R-deleted SARS-CoV-2-specific furin motif (EpiGentek), and His-tagged SARS-CoV-2 S1 RBD protein lacking the S1/S2 boundary furin site (EpiGentek) were added at a concentration of 10 ng/well (prepared with PBS) to the blocked (2% BSA) Ni-NTA-coated strips and incubated for 1 h at 37 °C. After washing the strips for 2 times with PBS-T, fbAB (50 μl) was added at a 1:5000 dilution (in PBS-T) and incubated for 1 h at RT. After washing for 3 times, anti-rabbit IgG-HRP (50 μl, 1:2000 dilution in PBS-T) was added and incubated for 30 min at RT. After washing for 4 times, 100 μl of TMB solution were added per well and blue color development was monitored for 2–10 min. The reaction was stopped with an equal volume of 1 M HCl and the optical density was measured with a microplate reader at a wavelength of 450 nm.

2.5. Immunoprecipitation by fbAB

fbAB was coated onto the 8-well polystyrene microplate strips at a concentration of 200 ng/well with 0.1 M $NaCO_3$. The strips were incubated for 2 h at 37 °C for coating, washed for 3 times with PBS-T, and then blocked with 2% BSA (in PBS) for 1 h at 37 °C. After washing the strips for 3 times, His-tagged SARS-CoV-2 protein containing the S1/S2 boundary furin site or His-tagged peptide containing the SARS-CoV-2-specific furin motif were added at different concentrations (prepared with PBS) to the fbAB-coated wells and incubated for 2 h at RT. After washing for 3 times, Ni-NTA-HRP (Millipore) (50 μl, 1:4000 dilution in PBS-T) was added and incubated for 30 min at RT. After washing for 4 times, 100 μl of TMB solution were added per well and blue color development was monitored for 2–10 min. The reaction was stopped with an equal volume of 1 M HCl and the optical density was measured with a microplate reader at a wavelength of 450 nm.

2.6. fbAB blockage of furin-mediated cleavage

Peptides (EpiGentek) containing the wild type, mutant (P681R and R683Q), and triple R-deleted SARS-CoV-2-specific furin motif and tagged with His- and biotin at the N- and C-terminals, respectively, were added at a concentration of 10 ng/well (prepared with PBS) to the blocked (2% BSA) Ni-NTA-coated strips and incubated for 1 h at RT. After washing the strips for 3 times with PBS-T, fbAB was added at a concentration of 200 ng/well (prepared with PBS-T) and incubated for 1 h at 37 °C. A SARS-CoV-2 neutralization antibody (EpiGentek), which targets the spike RBD, was used as a control. After washing for 3 times, purified proprotein convertase furin (New England Biolabs) was added at different concentrations (8–16 ng/well) and incubated for 25 min at 37 °C. Protease cleavage (PC) assay buffer (EpiGentek) was used to prepare the furin solutions. After washing for 4 times, streptavidin-HRP (100 μl, 1:5000 dilution in PBS-T) was added and incubated for 15 min at RT. After washing for 4 times, 100 μl of TMB solution were added per well and blue color development was monitored for 2–10 min. The reaction was stopped with an equal volume of 1 M HCl and the optical density was measured with a microplate reader at a wavelength of 450 nm.

2.7. fbAB blockage of trypsin-mediated cleavage

His- and biotin-tagged peptides containing the wild type, mutant (P681R and R683Q), and triple R-deleted SARS-CoV-2-specific furin motif were added at a concentration of 10 ng/well (prepared with PBS) to the blocked (2% BSA) Ni-NTA-coated wells of the 8-well microplate strips and incubated for 1 h at RT. After washing the strips for 3 times with PBS-T, fbAB was added at a concentration of 200 ng/well (prepared with PBS-T) and incubated for 1 h at 37 °C. After washing for 3 times,

serine protease trypsin (Sigma) was added at 20 ng/well (prepared with PC assay buffer) and incubated for 25 min at 37 °C. After washing for 4 times, streptavidin-HRP (100 µl, 1:5000 dilution in PBS-T) was added and incubated for 15 min at RT. After washing for 4 times, 100 µl of TMB solution were added per well and blue color development was monitored for 2–10 min. The reaction was stopped with an equal volume of 1 M HCl and the optical density was measured with a microplate reader at a wavelength of 450 nm.

2.8. fbAB blockage of human nasal swab-mediated cleavage

Collection of nasal swab samples from healthy uninfected volunteers was in accordance with the standard CDC nasal swab collection protocol. The collected samples were released into 300 µl of PC assay buffer by rotating the swab in the buffer for 30 s.

His- and biotin-tagged peptide containing the SARS-CoV-2-specific furin motif was added at a concentration of 10 ng/well (prepared with PBS) to the blocked (2% BSA) Ni-NTA-coated wells of the 8-well microplate strips and incubated for 1 h at RT. After washing the strips for 3 times with PBS-T, fbAB was added at a concentration of 200 ng/well (prepared with PBS-T) and incubated for 1 h at 37 °C. After washing for 3 times, 20–30 µl of nasal swab sample solution were added per well and incubated for 25 min at 37 °C. After washing for 4 times, streptavidin-HRP (100 µl, 1:5000 dilution in PBS-T) was added and incubated for 15 min at RT. After washing for 4 times, 100 µl of TMB solution were added per well and blue color development was monitored for 2–10 min. The reaction was stopped with an equal volume of 1 M HCl and the optical density was measured with a microplate reader at a wavelength of 450 nm.

2.9. fbAB blockage of spike-ACE2 binding

Untagged SARS-CoV-2 spike protein (GenScript) containing the S1/S2 boundary furin site was coated onto the high protein binding, polystyrene, 8-well microplate strips at a concentration of 50 ng/well with 0.1 M $NaCO_3$. The strips were incubated for 2 h at 37 °C for coating and then blocked with 2% BSA (in PBS) for 1 h at 37 °C. After washing the strips for 3 times with PBS-T, fbAB was added into the wells at the indicated concentrations (prepared with PBS-T) and incubated for 1 h at 37 °C. After washing for 3 times, purified His-tagged ACE2 (EpiGentek) was added at a concentration of 100 ng/well (prepared with PBS) and incubated for 1 h at 37 °C. After washing for 3 times, Ni-NTA-HRP (50 µl, 1:4000 dilution in PBS-T) was added and incubated for 30 min RT. After washing for 4 times, 100 µl of TMB solution were added per well and blue color development was monitored for 2–10 min. The reaction was stopped with an equal volume of 1 M HCl and the optical density was measured with a microplate reader at a wavelength of 450 nm.

2.10. Statistical analysis

Data are presented as means ± SEM from 2 independent replicates. Differences between means were analyzed by two-tailed *t*-test.

The cleavage percentage of enzyme-treated samples incubated with or without fbAB was calculated as follows:

$$Cleavage\% = \left(1 - \frac{OD\ treated}{OD\ untreated\ control}\right) \times 100\%$$

The percent ACE2 binding activity of spike protein incubated with different concentrations of fbAB was calculated as follows:

$$\%ACE2\ binding\ activity = \left(\frac{OD\ with\ fbAB}{OD\ without\ fbAB}\right) \times 100\%$$

3. Results

After generation of furin site blocking antibody (fbAB) raised against an antigen consisting of the 20 amino acid SARS-CoV-2-specific furin motif (Fig. 1), the fbAB titer was evaluated using an ELISA-based colorimetric detection system with antigen-coated microplates. As shown in Fig. 2, when compared with normal serum, fbAB purified from serum of antigen-injected host displayed a strong signal intensity (OD >2.5) at 8000X dilution. The optical density decreased linearly over successive 2-fold serial dilutions, but a high signal intensity (OD >1) was still observed for fbAB diluted as much as 128000X. The results indicate that high amounts of fbAB against the furin motif of SARS-CoV-2 spike protein could be generated from antigen-injected host and subsequently detected with this novel colorimetric assay.

The sensitivity of fbAB recognizing the S1/S2 boundary furin site of SARS-CoV-2 spike protein was determined by incubating fbAB in nickel-coated microplate wells bound with different amounts of His-tagged target protein. Capture of the well-bound target by fbAB was then measured colorimetrically using ELISA-based detection. As shown in Fig. 3, the target protein displayed a dose-response with signal intensity increasing linearly up to a concentration of 100 ng/well. As low as 0.05 ng/well of the protein was detected with this assay, indicating high sensitivity of fbAB for SARS-CoV-2-specific furin motif recognition.

The specificity of fbAB-spike interaction was assessed by incubating antibody in wells coated with either: SARS-CoV-2 spike protein containing the S1/S2 boundary furin site; peptides containing the wild type, mutant (P681R and R683Q), and triple R-deleted SARS-CoV-2-specific furin motif; or SARS-CoV-2 S1 RBD protein. As shown in Fig. 4, fbAB displayed a strong binding interaction with the wild type furin cleavage site of both spike protein and peptide. The SARS-CoV-2 S1 RBD protein, which lacks the S1/S2 boundary furin site, failed to elicit a detectable signal. An antibody binding affinity test showed that mutation and deletion of the core furin cleavage region caused only a slight decrease in binding affinity (Supplementary Figure S1). The K_D associated with P681R mutation, R683Q mutation, and triple R deletion is 1.1, 1.8, and 1.5 nM, respectively, compared with 1.0 nM for wild type. Thus, the interaction was highly specific for both wide type and mutant/deletion peptides.

As the core region modifications did not significantly affect the binding of fbAB, we further examined whether the flanking solvent-accessible portion of the SARS-CoV-2 furin cleavage site plays a role in binding of fbAB. Either the C-terminal portion (P4-P6') or N-terminal portion (P14-P1) was removed by trypsin cleavage, and then fbAB antibody binding was determined. It was shown that peptide with N-terminal-flanking solvent-accessible regions allowed the antibody binding to be up to 71% of wild type peptide binding (Supplementary Figure S2). With C-terminal-flanking solvent-accessible regions, the antibody binding was about 57% of wild type peptide binding. These results suggest that the flanking solvent-accessible portion of the SARS-

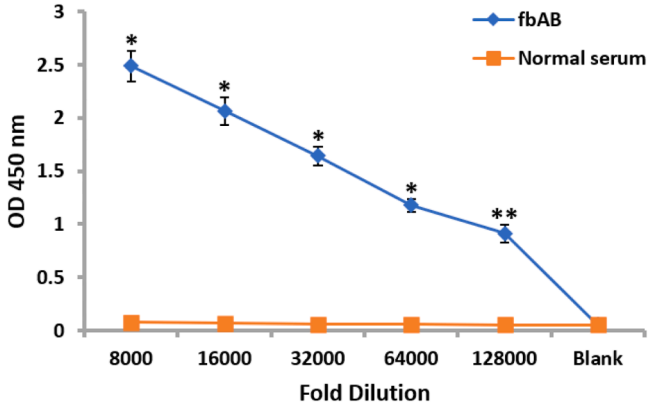

Fig. 2. fbAB titer of recognizing the antigen containing the SARS-CoV-2-specific furin motif. Antigen concentration = 200 ng/well. Data are presented as means ± SEM from 2 independent replicates. *$p < 0.005$; **$p < 0.01$.

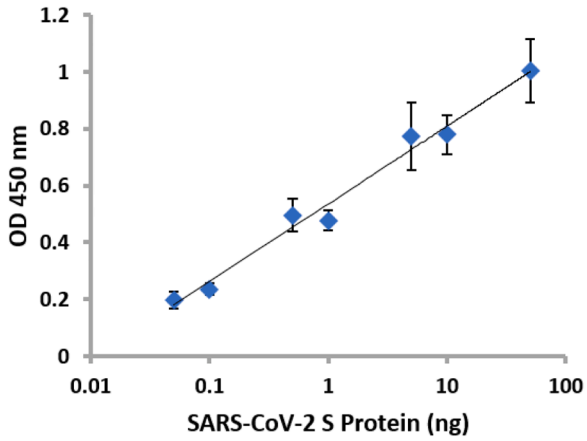

Fig. 3. Sensitivity of fbAB recognizing the antigen containing the SARS-CoV-2-specific furin motif. Data are presented as means ± SEM from 2 independent replicates. Blank OD = 0.063 ± 0.002.

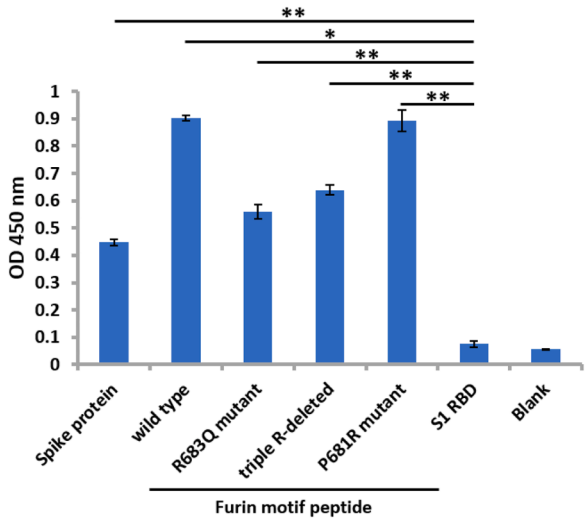

Fig. 4. Specificity of fbAB recognizing the SARS-CoV-2 spike protein containing the S1/S2 boundary furin site or peptide containing the SARS-CoV-2-specific furin motif (with or without modification of the wild type motif sequence). SARS-CoV-2 S1 RBD protein lacking the S1/S2 boundary furin site served as a negative control. Data are presented as means ± SEM from 2 independent replicates. *$p < 0.0005$; **$p < 0.005$.

CoV-2 furin cleavage site is essentially required for fbAB binding.

The S protein and peptide were further used to assess the immunoprecipitation efficiency of fbAB in antibody-coated wells. Fig. 5 shows the efficient immunocapture of both S protein and peptide by fbAB in a concentration-dependent manner. The results indicate that synthesized peptide is the same as biological S protein for use as an assay substrate, as both the peptide and full-length S protein were strongly bound by fbAB. Thus, synthesized peptide was utilized in the follow-up cleavage blockage assays.

Next, fbAB blockage of SARS-CoV-2 furin motif cleavage via enzymatic activity was examined. Dual His- and biotin-tagged peptide containing the SARS-CoV-2-specific furin motif was bound to Ni-coated microplate wells. The wells were then incubated with fbAB, followed by exposure to either of two different enzymes (furin, trypsin) or human nasal swab sample. Cleavage at the furin motif will remove the C-terminal portion of the peptide, resulting in inhibition of streptavidin-HRP binding to biotin and reduced signal intensity. As shown in Fig. 6A, fbAB effectively blocked the cleavage of the wild type and P681R SARS-CoV-2 furin motif by purified furin enzyme at 8 ng/well. A higher

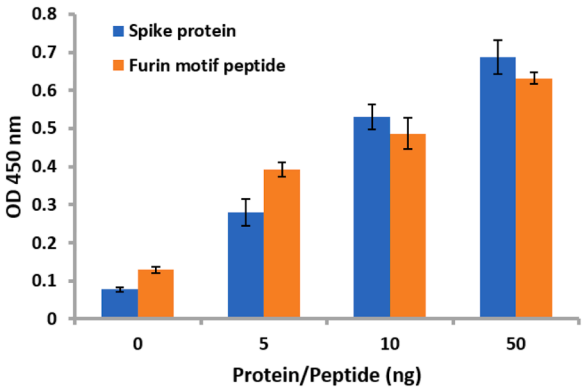

Fig. 5. Immunoprecipitation by fbAB of the SARS-CoV-2 protein containing the S1/S2 boundary furin site and peptide containing the SARS-CoV-2 specific furin motif. Data are presented as means ± SEM from 2 independent replicates.

concentration (16 ng/well) of furin enzyme increased cleavage of the wild type and P681R SARS-CoV-2 furin cleavage site, and fbAB was found to effectively reduce the cleavage by furin at this concentration as well (Fig. 6B). Peptide pre-incubated with fbAB prior to peptide binding to the assay wells was similarly afforded protection against cleavage by furin (Supplementary Figure S3). By comparison, SARS-CoV-2 neutralization antibody (SnAB), which was used as a control and targets the spike RBD, showed minimal blocking of furin-mediated cleavage (Fig. 6A). fbAB also downregulated cleavage mediated by the serine protease trypsin (Fig. 7), although to a lesser extent when compared with furin. PCs from human nasal swab samples displayed a high cleavage percentage (~80%) of the furin motif, which was decreased by approximately 20–26% in the presence of fbAB (Fig. 8).

As cleavage of the S protein at the S1/S2 site is required for SARS-CoV-2 binding to the host ACE2 receptor for cell entry, we tested the effect of fbAB on spike-ACE2 interaction in SARS-CoV-2 spike protein-coated wells. As shown in Fig. 9, fbAB blocked the binding of ACE2 to S protein in a dose-dependent manner, with >60% of ACE2 binding activity diminished at an fbAB dose of 40 nM and almost complete inhibition of spike-ACE2 binding at 80 nM of antibody.

4. Discussion

During infection, the cell entry mechanism of SARS-CoV-2 involves direct contact with the host ACE2 receptor, facilitated by the RBD within the S1 subunit of the S protein, and proteolytic cleavage of the S1/S2 multibasic cleavage site by the cell surface transmembrane protease serine 2 (TMPRSS2) and cellular cathepsin L [2,14,15]. The S1/S2 junction also harbors a unique furin cleavage site that can be cleaved by furin and other PCs in lieu of TMPRSS2/cathepsin L activity, which may enhance infectivity [13,16]. A recent study showed that a furin cleavage site-deleted SARS-CoV-2 mutant exhibited reduced replication in human respiratory cells and attenuation of viral pathogenesis in vivo models [17]. In contrast, the mutation of P681H (Alpha variant) and P681R (Delta variant) significantly increased viral replication and transmission [10,18], largely due to increased cleavage of S1/S2 site by furin enzyme [19]. The widespread expression of furin, especially in the human lung [20,21], makes the furin cleavage site an ideal target for therapeutic intervention.

Through use of a synthesized peptide containing the SARS-CoV-specific furin cleavage sequence (entire 20 amino acid motif, Fig. 1) as an antigen, a high titer antibody was generated with high sensitivity and specificity for the S1/S2 boundary furin site. This furin site blocking antibody (fbAB) was further examined using a series of innovative ELISA-based colorimetric assays to rapidly and reliably measure its efficiency at blocking cleavage and receptor interaction. fbAB demonstrated effective blockage of SARS-CoV-2 wide type and/or P681R S1/S2

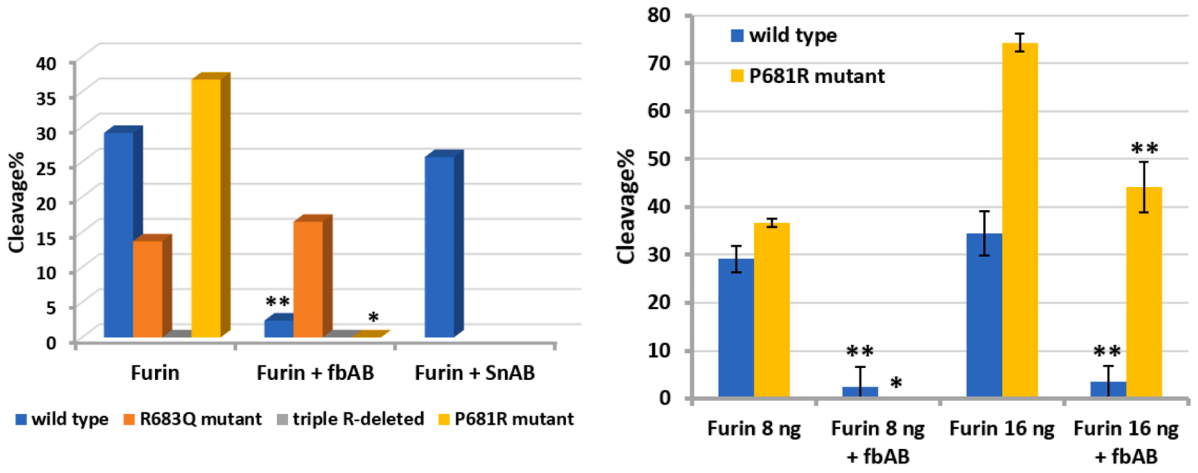

Fig. 6. fbAB blockage of wild type and mutant SARS-CoV-2 furin motif cleavage by furin enzyme. Furin concentration = 8 ng/well (A) and 8–16 ng/well (B). fbAB and spike protein neutralization antibody (SnAB) concentration = 200 ng/well. Data are presented as means ± SEM from 2 independent replicates. *$p < 0.02$; **$p < 0.05$; Furin group versus Furin + fbAB group.

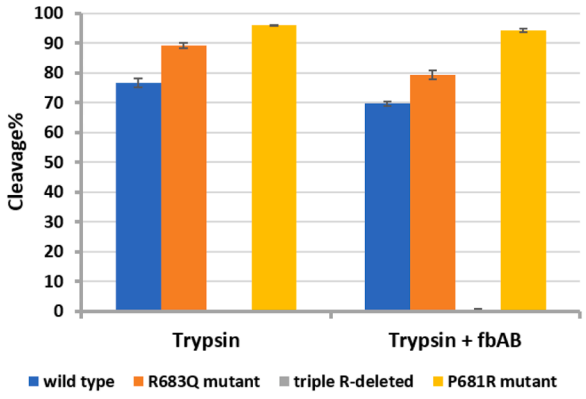

Fig. 7. fbAB blockage of wild type and mutant SARS-CoV-2 furin motif cleavage by facilitating protease trypsin. Trypsin concentration = 20 ng/well. fbAB concentration = 200 ng/well. Data are presented as means ± SEM from 2 independent replicates. *$p < 0.05$; Trypsin group versus Trypsin + fbAB group.

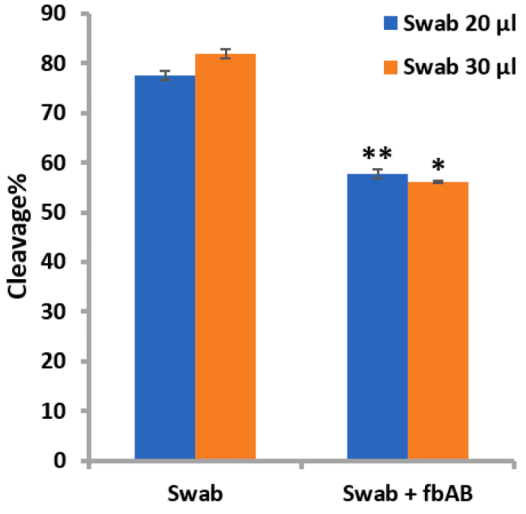

Fig. 8. fbAB blockage of SARS-CoV-2 furin motif cleavage by human nasal swab sample. Human nasal swab sample was released into 300 µl of furin assay buffer and 20–30 µl of sample solution was used for the assay. fbAB concentration = 200 ng/well. Data are presented as means ± SEM from 2 independent replicates. *$p < 0.002$; **$p < 0.005$; Swab group versus Swab + fbAB group.

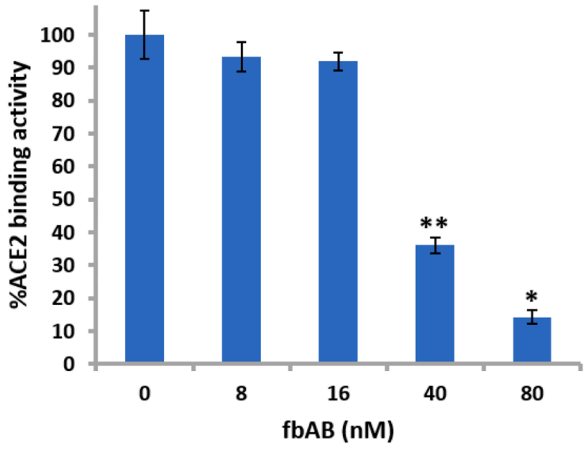

Fig. 9. Reduction of ACE2 binding to SARS-CoV-2 spike protein by fbAB blocking the SARS-CoV-2 furin motif at different concentrations. Coated SARS-CoV-2 spike protein concentration = 50 ng/well. ACE2 concentration = 100 ng/well. Data are presented as means ± SEM from 2 independent replicates. *$p < 0.01$; **$p < 0.02$; no treatment group versus fbAB treatment group.

furin site cleavage caused by purified furin enzyme, the serine protease trypsin, and human nasal swab specimens. It was shown that in both asymptomatic and symptomatic COVID-19 patients, nasal samples have yielded higher viral loads than throat samples [22], indicating the nasal epithelium as a portal for initial infection and transmission and as a dominant location for viral replication through pre-activation by PCs from both host and bacteria in the nasal cavity. Based on our results, human nasal swab specimens yielded 80% cleavage of the assay substrate containing the SARS-CoV-2-specific furin motif, confirming this sample type as a valid biological source of abundant PC activity.

The mutation of ^{P}681 (non-polar proline) to positively charged ^{R}681 (arginine) to form multibasic amino acid sites could further increase S1/S2 boundary cleavage, thereby increasing viral replicates in human airway and transmission [10]. The P681R mutation is a hallmark of the Delta variant, the dominant strain of the COVID-19 global pandemic, and leads to increased resistance of SARS-CoV-2 to wild type spike vaccine [23]. Thus, inhibition of SARS-CoV-2 cleavage of the furin site containing P681R would allow for the reduction of furin site cleavage-based activation of SARS-CoV-2 Delta variant spike protein, thereby decreasing viral binding to ACE2, cell-cell fusion, and viral entry into human cells. Based on our results, peptide containing the P681R

mutant SARS-CoV-2-specific furin motif indeed was more susceptible to cleavage by furin than the wild type site, and fbAB treatment was able to significantly reduce the cleavage percentage.

It should be noted that in addition to blocking furin-mediated cleavage of bound target, fbAB pre-incubated with peptide containing the SARS-CoV-2-specific furin motif, before immobilization on the well surface, was also effective at inhibiting enzyme cleavage. As virus particles are mobile targets within the systemic circulation, it was necessary to confirm that antibody interaction with unbound target in suspension status could reduce formation of cleaved product as seen with immobile peptide.

Given the importance of the spike/furin/ACE2 signal axis in the infection pathway of SARS-CoV-2, the ability of fbAB to disrupt binding interaction between S protein and its host receptor is critical to attenuating the spread of disease. fbAB demonstrated very high potency in blocking the binding of ACE2 to S protein-coated microplate wells, effectively reducing the percentage of receptor binding activity to a nearly undetectable level at a submicromolar antibody concentration.

Current approaches to blocking or reducing furin site cleavage of target proteins are predicated on the direct inhibition of furin or furin-like enzymes. Such inhibition is generally achieved by naturally-occurring macromolecular protein-based inhibitors (e.g., serpin A1-antitrypsin) or small molecule chemical inhibitors (e.g., pure peptide, peptide mimetics, and nonpeptidic compounds). As these inhibitors are selective for the proteases themselves rather than specific sites of proteolytic activity, their inhibitory effect is limited with regard to preventing furin site cleavage exclusively at a precise location such as the S protein of SARS-CoV-2. Furthermore, furin and furin-related PCs are widely distributed in various human tissues. The inhibition of host proteases could non-specifically damage the normal functionality of proteins that require activation by these enzymes. Therefore, our strategy of implementing an antibody to expressly block the SARS-CoV-2-specific furin site from cleavage by furin and facilitating proteases would be a selective option in controlling the activation of SARS-CoV-2 spike protein and the spread of the virus.

Funding

This study was funded by EpiGentek.

Declaration of Competing Interest

The authors have no competing interests to declare.

Supplementary materials

Supplementary material associated with this article can be found, in the online version, at doi:10.1016/j.imlet.2022.01.002.

References

[1] N. Zhu, D. Zhang, W. Wang, X. Li, B. Yang, J. Song, X. Zhao, B. Huang, W. Shi, R. Lu, P. Niu, F. Zhan, X. Ma, D. Wang, W. Xu, G. Wu, G.F. Gao, W. Tan, China Novel Coronavirus Investigating and Research Team, A novel coronavirus from patients with pneumonia in China, 2019, N. Engl. J. Med. 382 (8) (2020 Feb 20) 727–733, https://doi.org/10.1056/NEJMoa2001017. Epub 2020 Jan 24. PMID: 31978945; PMCID: PMC7092803.

[2] F. Wu, S. Zhao, B. Yu, Y.M. Chen, W. Wang, Z.G. Song, Y. Hu, Z.W. Tao, J.H. Tian, Y.Y. Pei, M.L. Yuan, Y.L. Zhang, F.H. Dai, Y. Liu, Q.M. Wang, J.J. Zheng, L. Xu, E. C. Holmes, Y.Z. Zhang, A new coronavirus associated with human respiratory disease in China, Nature 579 (7798) (2020 Mar) 265–269, https://doi.org/10.1038/s41586-020-2008-3. Epub 2020 Feb 3. Erratum in: Nature. 2020 Apr;580 (7803):E7. PMID: 32015508; PMCID: PMC7094943.

[3] J. Lan, J. Ge, J. Yu, S. Shan, H. Zhou, S. Fan, Q. Zhang, X. Shi, Q. Wang, L. Zhang, X. Wang, Structure of the SARS-CoV-2 spike receptor-binding domain bound to the ACE2 receptor, Nature 581 (7807) (2020 May) 215–220, https://doi.org/10.1038/s41586-020-2180-5. Epub 2020 Mar 30. PMID: 32225176.

[4] A.C. Walls, Y.J. Park, M.A. Tortorici, A. Wall, A.T. McGuire, D. Veesler, Structure, function, and antigenicity of the SARS-CoV-2 spike glycoprotein, Cell 181 (2) (2020 Apr 16) 281–292, https://doi.org/10.1016/j.cell.2020.02.058. .e6Epub 2020 Mar 9. Erratum in: Cell. 2020 Dec 10;183(6):1735. PMID: 32155444; PMCID: PMC7102599.

[5] S. Tian, Q. Huang, Y. Fang, Wu J. FurinDB, A database of 20-residue furin cleavage site motifs, substrates and their associated drugs, Int. J. Mol. Sci. 12 (2) (2011 Feb 8) 1060–1065, https://doi.org/10.3390/ijms12021060. PMID: 21541042; PMCID: PMC3083689.

[6] B. Coutard, C. Valle, X. de Lamballerie, B. Canard, N.G. Seidah, E. Decroly, The spike glycoprotein of the new coronavirus 2019-nCoV contains a furin-like cleavage site absent in CoV of the same clade, Antiviral Res 176 (2020 Apr), 104742, https://doi.org/10.1016/j.antiviral.2020.104742. Epub 2020 Feb 10. PMID: 32057769; PMCID: PMC7114094.

[7] M. Örd, I. Faustova, M. Loog, The sequence at Spike S1/S2 site enables cleavage by furin and phospho-regulation in SARS-CoV2 but not in SARS-CoV1 or MERS-CoV, Sci. Rep. 10 (1) (2020 Oct 9) 16944, https://doi.org/10.1038/s41598-020-74101-0. PMID: 33037310; PMCID: PMC7547067.

[8] L. Dai, G.F. Gao, Viral targets for vaccines against COVID-19, Nat. Rev. Immunol. 21 (2) (2021 Feb) 73–82, https://doi.org/10.1038/s41577-020-00480-0. Epub 2020 Dec 18. PMID: 33340022; PMCID: PMC7747004.

[9] P. Lee, C.U. Kim, S.H. Seo, D.J. Kim, Current Status of COVID-19 vaccine development: focusing on antigen design and clinical trials on later stages, Immune Netw. 21 (1) (2021 Feb 26) e4, https://doi.org/10.4110/in.2021.21.e4. PMID: 33728097; PMCID: PMC7937514.

[10] Akatsuki Saito, Takashi Irie, Rigel Suzuki, Tadashi Maemura, Hesham Nasser, Keiya Uriu, Yusuke Kosugi, Kotaro Shirakawa, Kenji Sadamasu, Izumi Kimura, Jumpei Ito, Jiaqi Wu, Kiyoko Iwatsuki-Horimoto, Mutsumi Ito, Seiya Yamayoshi, Seiya Ozono, Erika P Butlertanaka, Yuri L Tanaka, Ryo Shimizu, Kenta Shimizu, Kumiko Yoshimatsu, Ryoko Kawabata, Takemasa Sakaguchi, Kenzo Tokunaga, Isao Yoshida, Hiroyuki Asakura, Mami Nagashima, Yasuhiro Kazuma, Ryosuke Nomura, Yoshihito Horisawa, Kazuhisa Yoshimura, Akifumi Takaori-Kondo, Masaki Imai, , The Genotype to Phenotype Japan (G2P-Japan) Consortium, So Nakagawa, Terumasa Ikeda, Takasuke Fukuhara, Yoshihiro Kawaoka, Kei Sato, SARS-CoV-2 spike P681R mutation, a hallmark of the Delta variant, enhances viral fusogenicity and pathogenicity, bioRxiv (2021.06.17), 448820, https://doi.org/10.1101/2021.06.17.448820.

[11] Z. Liu, H. Zheng, H. Lin, M. Li, R. Yuan, J. Peng, Q. Xiong, J. Sun, B. Li, J. Wu, L. Yi, X. Peng, H. Zhang, W. Zhang, R.J.G. Hulswit, N. Loman, A. Rambaut, C. Ke, T. A. Bowden, O.G. Pybus, J. Lu, Identification of common deletions in the spike protein of severe acute respiratory syndrome coronavirus 2, J. Virol. 94 (17) (2020 Aug 17) e00720–e00790, https://doi.org/10.1128/JVI.00790-20. PMID: 32571797; PMCID: PMC7431800.

[12] W. Garten, Characterization of Proprotein Convertases and their involvement in virus propagation, Activation of Viruses by Host Proteases (2018 Feb 16) 205–248, https://doi.org/10.1007/978-3-319-75474-1_9. PMCID: PMC7122180.

[13] M. Hoffmann, H. Kleine-Weber, S. Pöhlmann, A multibasic cleavage site in the spike protein of SARS-CoV-2 is essential for infection of human lung cells, Mol Cell 78 (4) (2020 May 21) 779–784.e5, https://doi.org/10.1016/j.molcel.2020.04.022. Epub 2020 May 1. PMID: 32362314; PMCID: PMC7194065.

[14] M. Hoffmann, H. Kleine-Weber, S. Schroeder, N. Krüger, T. Herrler, S. Erichsen, T. S. Schiergens, G. Herrler, N.H. Wu, A. Nitsche, M.A. Müller, C. Drosten, S. Pöhlmann, SARS-CoV-2 cell entry depends on ACE2 and TMPRSS2 and is blocked by a clinically proven protease inhibitor, Cell. 181 (2) (2020 Apr 16) 271–280.e8, https://doi.org/10.1016/j.cell.2020.02.052. Epub 2020 Mar 5. PMID: 32142651; PMCID: PMC7102627.

[15] P. Zhou, X.L. Yang, X.G. Wang, B. Hu, L. Zhang, W. Zhang, H.R. Si, Y. Zhu, B. Li, C. L. Huang, H.D. Chen, J. Chen, Y. Luo, H. Guo, R.D. Jiang, M.Q. Liu, Y. Chen, X. R. Shen, X. Wang, X.S. Zheng, K. Zhao, Q.J. Chen, F. Deng, L.L. Liu, B. Yan, F. X. Zhan, Y.Y. Wang, G.F. Xiao, Z.L. Shi, A pneumonia outbreak associated with a new coronavirus of probable bat origin, Nature 579 (7798) (2020 Mar) 270–273, https://doi.org/10.1038/s41586-020-2012-7. Epub 2020 Feb 3. PMID: 32015507; PMCID: PMC7095418.

[16] J. Shang, Y. Wan, C. Luo, G. Ye, Q. Geng, A. Auerbach, F. Li, Cell entry mechanisms of SARS-CoV-2, Proc. Natl. Acad. Sci. U S A. 117 (21) (2020 May 26) 11727–11734, https://doi.org/10.1073/pnas.2003138117. Epub 2020 May 6. PMID: 32376634; PMCID: PMC7260975.

[17] B.A. Johnson, X. Xie, A.L. Bailey, B. Kalveram, K.G. Lokugamage, A. Muruato, J. Zou, X. Zhang, T. Juelich, J.K. Smith, L. Zhang, N. Bopp, C. Schindewolf, M. Vu, A. Vanderheiden, E.S. Winkler, D. Swetnam, J.A. Plante, P. Aguilar, K.S. Plante, V. Popov, B. Lee, S.C. Weaver, M.S. Suthar, A.L. Routh, P. Ren, Z. Ku, Z. An, K. Debbink, M.S. Diamond, P.Y. Shi, A.N. Freiberg, V.D. Menachery, Loss of furin cleavage site attenuates SARS-CoV-2 pathogenesis, Nature (2021 Jan 25), https://doi.org/10.1038/s41586-021-03237-4. Epub ahead of print. PMID: 33494095.

[18] A. Mohammad, J. Abubaker, F. Al-Mulla, Structural modelling of SARS-CoV-2 alpha variant (B.1.1.7) suggests enhanced furin binding and infectivity, Virus Res. 303 (2021 Oct 2), 198522, https://doi.org/10.1016/j.virusres.2021.198522. Epub 2021 Jul 24. PMID: 34314772; PMCID: PMC8310422.

[19] Yang Liu, Jianying Liu, Bryan A. Johnson, Hongjie Xia, Zhiqiang Ku, Craig Schindewolf, Steven G. Widen, Zhiqiang An, Scott C. Weaver, Vineet D. Menachery, Xuping Xie, Pei-Yong Shi, Delta spike P681R mutation enhances SARS-CoV-2 fitness over Alpha variant, bioRxiv (2021.08.12), 456173, https://doi.org/10.1101/2021.08.12.456173.

[20] K.E. Follis, J. York, J.H. Nunberg, Furin cleavage of the SARS coronavirus spike glycoprotein enhances cell-cell fusion but does not affect virion entry, Virology 350 (2) (2006 Jul 5) 358–369, https://doi.org/10.1016/j.virol.2006.02.003. Epub 2006 Mar 7. PMID: 16519916; PMCID: PMC7111780.

[21] S. Lukassen, R.L. Chua, T. Trefzer, N.C. Kahn, M.A. Schneider, T. Muley, H. Winter, M. Meister, C. Veith, A.W. Boots, B.P. Hennig, M. Kreuter, C. Conrad, R. Eils, SARS-

CoV-2 receptor ACE2 and TMPRSS2 are primarily expressed in bronchial transient secretory cells, EMBO J. 39 (10) (2020 May 18), e105114, https://doi.org/10.15252/embj.20105114. Epub 2020 Apr 14. PMID: 32246845; PMCID: PMC7232010.

[22] W. Sungnak, N. Huang, C. Bécavin, M. Berg, R. Queen, M. Litvinukova, C. Talavera-López, H. Maatz, D. Reichart, F. Sampaziotis, K.B. Worlock, M. Yoshida, J. L. Barnes, H.C.A. Lung Biological Network, SARS-CoV-2 entry factors are highly expressed in nasal epithelial cells together with innate immune genes, Nat. Med. 26 (5) (2020 May) 681–687, https://doi.org/10.1038/s41591-020-0868-6. Epub 2020 Apr 23. PMID: 32327758.

[23] D. Planas, D. Veyer, A. Baidaliuk, I. Staropoli, F. Guivel-Benhassine, M.M. Rajah, C. Planchais, F. Porrot, N. Robillard, J. Puech, M. Prot, F. Gallais, P. Gantner, A. Velay, J. Le Guen, N. Kassis-Chikhani, D. Edriss, L. Belec, A. Seve, L. Courtellemont, H. Péré, L. Hocqueloux, S. Fafi-Kremer, T. Prazuck, H. Mouquet, T. Bruel, E. Simon-Lorière, F.A. Rey, O Schwartz, Reduced sensitivity of SARS-CoV-2 variant Delta to antibody neutralization, Nature 596 (7871) (2021 Aug) 276–280, https://doi.org/10.1038/s41586-021-03777-9. Epub 2021 Jul 8. PMID: 34237773.